Global and Planetary Change 177 (2019) 1–9

Contents lists available at ScienceDirect

Global and Planetary Change

journal homepage: www.elsevier.com/locate/gloplacha

Research article

Climate versus demographic controls on water availability across India at 1.5 °C, 2.0 °C and 3.0 °C global warming levels

Riddhi Singh[a,*], Rohini Kumar[b]

[a] Indian Institute of Technology Bombay, Powai, Maharashtra, India
[b] UFZ-Helmholtz Centre for Environmental Research, Leipzig, Germany

ARTICLE INFO

Keywords:
Water availability
Climate change
Population
GCM
SSP
Budyko

ABSTRACT

Water resources across the globe are projected to undergo significant changes as climate and socio-economic conditions change. A policy relevant question thus arises: whether climate change or population change exerts a greater control on future freshwater resources of a region? Understanding the relative importance of these factors in affecting water availability can help guide prioritization of policy level interventions. In this study, we quantify the changes in mean annual per capita water availability (PCWA) across India under 1.5 °C, 2.0 °C, and 3.0 °C levels of global warming. We utilize projections of future climate from several general circulation models (GCMs) under three different representative concentration pathways (RCPs) along with projections of future population from five socio-economic pathways (SSPs). Using the estimated PCWA from these GCM–RCP–SSP combinations, we perform a sensitivity analysis to ascertain the relative importance of climatic (precipitation and temperature change) and demographic (population) factors in affecting per capita freshwater availability in a region. Our analysis shows that PCWA over India will decrease across all warming scenarios. In addition, a transition from the 1.5 °C warmer world to the 2.0 °C warmer world leads to a reduction in PCWA for a majority (92.8%) of regions across India. The number of people likely to face severe water stress (PCWA < 500 m^3/*year*/*capita*) under 1.5 °C, 2.0 °C, and 3.0 °C warming scenarios, are 354, 421, and 380 million, respectively. Sensitivity analysis indicated that changes in both population and mean annual precipitation are dominating factors controlling PCWA, depending upon the historical setting of the region. Regions with historically lower populations and lower aridity indices tend to be more sensitive to population changes. On the other hand, as historical population of a region increases, sensitivity to changing climate (mainly mean annual precipitation) increases. These results indicate the complex interactions between demographic and climatic changes that need to be accounted for in policies that aim to manage water scarcity by either controlling global warming or via socio-economic interventions.

1. Introduction

Many parts of the world currently face varying levels of water stress due to over-exploitation of surface water and groundwater resources [Rodell et al., 2018; U. N. Water, 2007]. Impending changes in climate and socio-economic patterns is poised to worsen the situation further. There are numerous studies that project the impact of climate change on future water availability at various spatial scales such as global, regional, and catchment-scale [Arnell, 2004; Schewe et al., 2014; Kummu et al., 2016; Mekonnen and Hoekstra, 2016; Krysanova and Hattermann, 2017]. These analyzes indicate that changes in future water availability is driven mainly by changes in future precipitation. Multi-model assessments employing various general circulation models (GCMs) and hydrological models further show that for several regions across the globe, projections of future freshwater availability are highly uncertain mainly due to disagreement in the nature of precipitation change [Schewe et al., 2014].

As regions are expected to undergo both socio-economic and climatic changes, a significant body of literature considers the impact of both factors on water availability. One of the first notable efforts in this direction is the work by Vörösmarty et al. (2000), who estimated the combined impact of climate and population change on global water resources. Subsequent studies highlighted the relative role of climatic and population changes in controlling water availability in a region [Vörösmarty et al., 2010; Arnell and Lloyd-Hughes, 2014; Gosling and Arnell, 2016]. These analyses account for possible changes in future population by employing projections from state-of-the-art socio-economic models. These joint assessments generally conclude that increase

* Corresponding author.
E-mail address: riddhi@civil.iitb.ac.in (R. Singh).

https://doi.org/10.1016/j.gloplacha.2019.03.006
Received 9 October 2018; Received in revised form 3 March 2019; Accepted 12 March 2019
Available online 18 March 2019
0921-8181/ © 2019 Elsevier B.V. All rights reserved.

in global water stress will in fact be primarily due to increasing population and a transition to more water intensive lifestyles, not climate change. The work by Wiltshire et al. (2013) explored an additional factor affecting water availability, the plant physiological response to carbon dioxide forcing. They find that generally increased carbon dioxide concentration will increase plant water use efficiency resulting in a net increase in runoff. However, when changing precipitation, temperature, population and plant physiological response are considered together, they also conclude that population increase is the most critical factor that will lead to increased water stress.

In most studies, projected water availability under different future periods is analyzed to assess how each factor may affect water stress. For example, Vörösmarty et al. (2000) compare the relative role of population and climate change by projecting water availability in specific future periods considering only climate change, then only population change, and finally by considering both factors together. Similarly, Arnell and Lloyd-Hughes (2014) estimate water stress related indicators for various combinations of climate and socio-economic scenarios. These results are then interpreted qualitatively to assess how climate and socio-economic changes may jointly affect water stress. In this study, we propose to use a recently developed novel sensitivity analysis method to formally quantify the relative impacts of climate and population change on water stress. Pianosi and Wagener (2015) propose a simple and efficient sensitivity analysis method to quantify the sensitivity of a dependent variable to various factors. The method is advantageous over others as it considers the probability density function of the dependent variable, as opposed to its variance, to estimate sensitivity. We propose a modification to this method so that it can be applied to estimate the sensitivity of a water stress metric to changing climate and population using only future projections of these independent variables.

In lieu of analyzing changes in water availability at the end-of-century or other fixed future time periods, assessing how water availability changes at various levels of global warming is perhaps more decision–relevant. For example, if precipitation in a region first increases mildly and then drastically, an end-of-century assessment might show a overall increase in water availability even though the region may go through water scarcity in the early phases of climate change. Thus, an assessment of water availability considering the trajectory of changing climate is crucial for water resources planning. Such assessments are even more relevant when we consider recent geo–political developments related to climate change mitigation and adaptation. The Paris agreement sets a long–term goal of limiting global mean temperature rise below 2.0 °C as compared to pre–industrial levels. In addition, it also indicates that limiting global warming below 1.5 °C may carry significant benefits [Schleussner et al., 2016]. In order to substantiate the need to limit global warming to 1.5 °C below pre–industrial levels, assessments are needed that compare the impacts of changing climate under 1.5 °C and 2.0 °C warming scenarios. Recent studies have reacted to this call by estimating water resources under 1.5 °C and 2.0 °C global warming levels in several regions such as China [Zhai et al., 2018], Europe [Donnelly et al., 2017; Marx et al., 2018], and selected large catchments across the globe [Gosling et al., 2017]. However, there is no such study that provides these projections specifically for India at a fine spatial resolution. Being a developing country poised to undergo spatially variable climate change and increases in population over the next few decades, it is important to understand how climate and population change will alter freshwater availability under different global warming levels.

Climate change impact assessments also differ in the employed indicator of water stress. Depending upon the goal of the analysis, the metric of interest can be mean annual runoff, duration of low flows, peak floods, etc. [Milly et al., 2005; Döll and Schmied, 2012; Gosling et al., 2017; Krysanova and Hattermann, 2017; Zhai et al., 2018]. Other analyses focus on assessing the number of people under water stress under different future climates [Vörösmarty et al., 2000; Arnell, 2004; Rockström et al., 2009; Schewe et al., 2014]. Water stress is estimated either as a ratio of demand to supply of freshwater [Vörösmarty et al., 2000; Haddeland et al., 2014; Mekonnen and Hoekstra, 2016], or as freshwater available per person [Arnell, 2004; Rockström et al., 2009; Gerten et al., 2011; Schewe et al., 2014]. Either choices have their advantages and limitations [Xu and Wu, 2017].

In this study, we adopt the second metric, freshwater available per person, to estimate changes in long–term water availability for India at different levels of global warming. We employ a recently developed probabilistic Budyko model that allows us to estimate water availability at a relatively fine spatial resolution by using in–situ and remote sensing based information [Singh and Kumar, 2015]. Using this framework, we estimate how freshwater available per person will change under various climate and population growth scenarios that are obtained from state-of-the-art climate and socio-economic models. We aim to address the following questions:

1. How does water stress vary under 1.5 °C, 2.0 °C, and 3.0 °C levels of global warming?
2. Is there an advantage for long–term water security of India if a transition to 2.0 °C warmer world from a 1.5 °C warmer world is prevented?
3. What is the role of population growth *vis* − *a*` − *vis* precipitation and temperature change in determining water stress?

2. Material and methods

The procedure followed to project mean annual per capita water availability (PCWA) under 1.5 °C, 2.0 °C and 3.0 °C increase in global mean temperature is shown in Fig. 1. First, observed data is used to constrain a probabilistic Budyko model, which can project the upper limit of renewable freshwater under future climates (Section 2.2). Following this, projections of climate and population for 1.5 °C, 2.0 °C

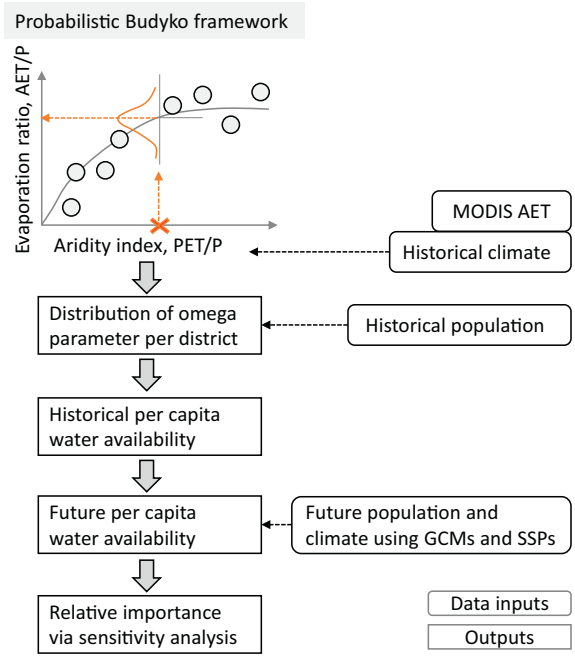

Fig. 1. The methodology used to estimate per capita water availability (PCWA). Long–term mean values of historical precipitation (P), potential evapotranspiration (PET), and actual evapotranspiration (AET) are assimilated within a probabilistic Budyko framework that predicts water availability as P–AET for each district. Using historical population data, PCWA is estimated. Future climate and population information from climate models (GCMs) and socio-economic models (SSPs) is then used to predict future PCWA followed by sensitivity analysis.

and 3.0 °C warming levels are derived (Section 2.3). These projections are then used to force the probabilistic Budyko model and estimate PCWA under various scenarios. The dataset on climate and population scenarios along with resultant PCWA is used to assess the sensitivity of PCWA to changes in long–term mean precipitation (*P*), long–term mean temperature (represented via potential evapotranspiration, *PET*) and population of spatial units across India (Section 2.4).

2.1. Data availability

For calibration of the Budyko model, we use a remote sensing based monthly actual evapotranspiration (*AET*) product, and ground based observations of precipitation and temperature. The *AET* product is available at a spatial resolution of 0.073° (≈ 8 km) from 1983 to 2006 [Zhang et al., 2009]. It has been cross-validated using eddy-covariance tower flux datasets and is available globally over a long time period, making it ideal for use in this study. The Indian Meteorological Department, Pune (India) provided monthly precipitation data for each district from 1901 to 2000, as well as daily maximum and minimum temperature data at a spatial resolution of (1 × 1)° for the period 1951–2000. We performed our analysis a decision–relevant spatial unit, termed districts in India. In total there are 637 districts over India with size varying between 10 and 86,064 km^2 with a median value of 3805 km^2 (Supplementary Fig. S1). An overlapping period of 1983–2000 was used to derive the long–term estimates of climatic variables. Districts with less than ten years of overlapping data or in violation of the physical constrains of atmospheric water supply (AE ≤ P) and demand (AE ≤ PE) were removed from the analysis.

Climate projections from a combination of general circulation models (GCMs) and representative concentration pathways (RCPs) are used to project future water availability. Five GCM outputs from the CMIP-5 database are analyzed: GFDL–ESM2M, HadGEM2–ES, IPSL–CM5A–LR, MIROC–ESM–CHEM, and NorESM1–M. Three RCPs are used: RCP2.6, RCP6.0, and RCP8.5, each resulting in corresponding level of radiative forcing (W/m^2) by 2100. Historical (1971–2100) and future (up to 2100) daily precipitation and temperature projections for each GCM–RCP combination are used. The climate datasets are available from the Inter-Sectoral Impact Model Intercomparison Project [Warszawski et al., 2014]. This is a global dataset downscaled using a bilinear interpolation scheme to a common 0.5°km horizontal resolution, and bias corrected using a trend-preserving approach based on the WATCH observation dataset [Hempel et al., 2013]. The grid size of downscaled and bias-corrected GCM data is roughly 50 km. As the area of districts are generally large (median: 3805 km^2, 10*th* percentile: 1354 km^2, Supplementary Fig. S1), for districts which encompass several GCM grids, area averaged P and PET are estimated from GCM outputs. For districts which fall under a single grid, the projected values are set as equal to the GCM grid value. We also note that the selected five GCMs cover a range of 0.55 (0.75) of the uncertainty of the entire CMIP5 ensemble for the precipitation (temperature) projections [McSweeney and Jones, 2016].

Future population projections for the world are based on five shared socioeconomic pathways(SSPs). We use SSP projected population data created by Jones and O'Neill (2016) available at a fine spatial resolution of 1/8° for the time period 2010–2100.The dataset is available from http://sedac.ciesin.columbia.edu. These SSPs are developed by accounting for different elements that exert control over demography such as land use, energy use, and emission pathways, as well as climate change vulnerability, impacts, and adaptation (Jones and O'Neill, 2017). As the population data is available at a resolution that is generally finer than the area of districts, future population for each district is obtained by aggregating various population grids together. For deriving average population estimates for an arbitrary time period from 2001 to 2100, the data is linearly interpolated at annual time steps and averaged. Historical baseline population data at district level is available from 2001 Census of India (available online at http://www.censusindia.gov.in/2011-common/census_data_2001.html).

2.2. The Probabilistic Budyko model

The Budyko approach exploits a well–known relationship between long–term averages of water and energy availability related indicators in a region [Budyko, 1958; Pike, 1964]. The Budyko function relates a climate indicator, the aridity index (*PET/P*) to a water availability indicator, the evaporation ratio (*AET/P*). Here, we employ a form of the Budyko curve with a firm physical basis:

$$\frac{AET}{P} = 1 + \frac{PET}{P} - \left(1 + \left(\frac{PET}{P}\right)^{\omega}\right)^{(1/\omega)}, \quad (1)$$

where, *PET* is estimated from temperature data [Hargreaves and Samani, 1985], and ω is a parameter inferred using observed data [Fu, 1981; Zhang et al., 2004]. Long–term water availability is then estimated as the difference between *P* and *AET*, assuming that changes in storage over multi–decadal time scales are zero [Singh and Kumar, 2015]. This is one way to estimate the upper limit of long–term freshwater availability in a region [Mishra et al., 2017]. Other sources of water like deep groundwater or derivation of freshwater from saline water in coastal regions are not accounted for in our estimates. To derive PCWA, $P - AET$ is divided by population estimate of each district.

ω encapsulates in itself the physical and socio-economic controls on precipitation partitioning between runoff and evapotranspiration at long time scales. We use observations of *P* and *PET* along with a satellite based *AET* product to calibrate ω for each district. The probabilistic model is then established following the methodology proposed by Greve et al. (2015), later applied by Singh and Kumar (2015) to Indian regions. A distribution of ω is obtained for each district by grouping ω values belonging to broader political regions together (see Supplementary Fig. S2 for a map of the political regions). This results in a range of water availability ($P - AET$) values for each district. The median value of projected $P - AET$ is used for analysis. Once calibrated using historical data, the probabilistic Budyko model allows us to estimate the impact of changing climatic conditions on long–term freshwater availability.

2.3. Future climate and population projections

We derive estimates of future water availability for three possible futures, each resulting in a global mean temperature increase of 1.5 °C, 2.0 °C and 3.0 °C. Specifically, we follow the procedure as described by Vautard et al. (2014), which has been also adopted in several recent climate change impact assessment studies [Jacob et al., 2018; Marx et al., 2018; Samaniego et al., 2018; Thober et al., 2018]. The 30-year period corresponding to 1971–2000 is taken as a reference and is approximately 0.46 °C warmer compared to preindustrial global mean temperature (1881–1910) based on different observational datasets [Vautard et al., 2014; Jacob et al., 2018]. Using this value as a reference, we identify 30-year periods for 15 GCM–RCP (5 GCMs, 3 RCPs) combinations in which the global mean temperature increases by 1.04 °C, 1.54 °C, and 2.54 °C, which in turn represent the conditions of 1.5 °C, 2.0 °C and 3.0 °C warmer worlds, respectively. We estimate changes in projected population for each district based on the projections of population from 5 SSPs for the 30–year window in which each GCM–RCP combination reaches a given level of warming. This procedure results in a total of 75 (5 × 3 × 5) possible climate and population change combinations for each district under each warming level. Across three warming levels, 225 (75 × 3) potential combinations of climate and population change scenarios can be obtained.

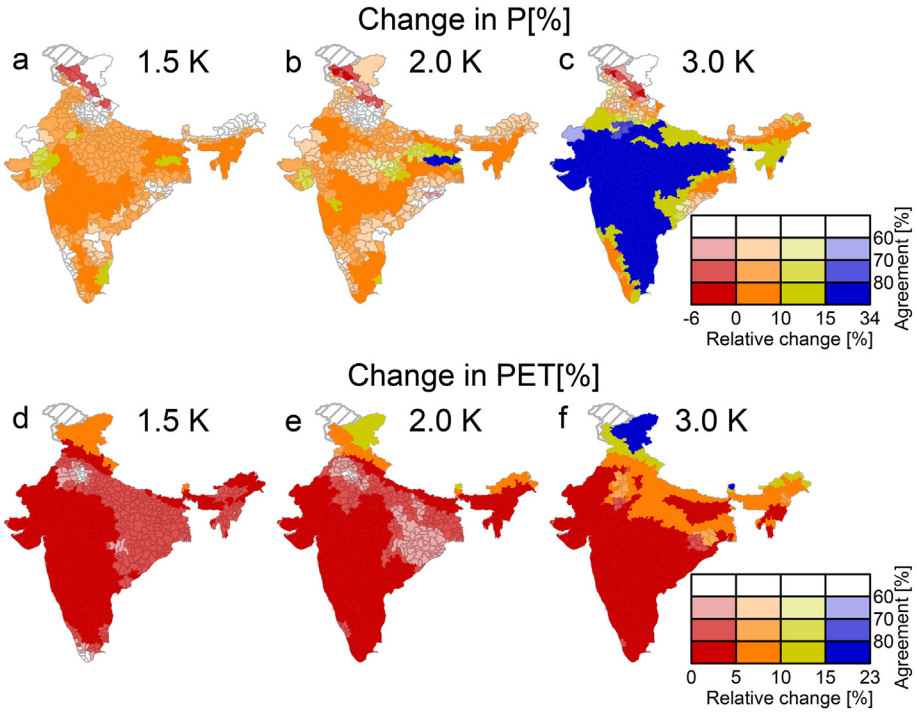

Fig. 2. Projections of median change in (a-c) long—term precipitation (*P*), and (d-f) long–term potential evapotranspiration (*PET*), across 5 GCMs and 3 RCPs for each district. The change is estimated for 30-year windows that result in a) 1.5 °C, b) 2.0 °C, and c) 3 °C rise in global mean temperature compared to pre-industrial levels. Color denotes the median of the change relative to the baseline values (1971–2000) across all GCM–RCP combinations. Transparency denotes the degree of agreement between different GCM–RCP combinations on the direction of change ranging from white (no agreement) to solid color (full agreement). Note that not all GCM–RCP combinations may result in a given warming level; these are ignored while estimating the median.

2.4. Sensitivity analysis

Understanding the relative importance of climate and population change on PCWA has significant policy relevance. Here, we assess the joint impact of these factors on PCWA by performing a sensitivity analysis that ascertains which of the three independent factors has most influence on future PCWA: *P*, *PET*, or population. Recall that we quantify PCWA, the dependent variable, for each of the three controlling factors across 225 possible futures. We use a recently developed sensitivity analysis technique to exploit this dataset and provide estimates of sensitivity of output variable to independent variables [Pianosi and Wagener, 2015]. We perform this exercise for each district, which allows us to explore the spatial variability of the most sensitive factors across the study domain.

Pianosi and Wagener (2015) propose an efficient and computationally inexpensive method to estimate sensitivity of an output variable, y, to various factors, x_i. Each subscript i corresponds to a factor and ranges from 1 to the number of independent factors, three in this case. The sensitivity index is a summary statistic based on the non-parametric measure, the Kolmogorov–Smirnof (K−S) statistic, that measures the distance between two CDFs as:

$$KS(x_i) = \max_y |F_y(y) - F_{y|x_i}(y)| \quad (2)$$

where $F_y(y)$ is the unconditional CDF of y, i.e., the CDF constructed using all values of y. $F_{y|xi}(y)$ is the conditional CDF of y when a factor, x_i is fixed at a certain value. If the unconditional CDF of y is very different from the conditional CDF of y, it implies that a substantial variation in y is due to x_i. A high KS–Statistic value indicates greater sensitivity to a factor x_i. In order to obtain an estimate of the KS–Statistic that is independent of the specific value at which x_i is fixed, the statistic is estimated across all possible values of x_i, and then a summary statistic is calculated. Thus, higher values of the summary statistic imply greater sensitivity of y to x_i and vice-versa.

In this study, like in many others that employ simulation modelling, the analytical derivation of the CDFs is not feasible and instead, empirical CDFs are employed as also recommended by Pianosi and Wagener (2015). Changes in each factor: *P*, *PET* and population, are divided into ten equally spaced bins, ranging from minimum to maximum projected value of change. The changes in climate and population along with corresponding values of PCWA within a bin are used to estimate the empirical conditional CDF, and the KS–Statistic thereafter. Finally, the median KS–Statistic is estimated across the ten bins and is used as a measure of sensitivity. Note that we do not perform any additional sampling of the factor space to estimate the sensitivity indices but use only 225 possible projections from various GCM–RCP–SSP combinations for each district. This allows us to estimate the sensitivity indices within decision–relevant ranges.

3. Results

3.1. Climate and population projections

GCMs vary in terms of model structures and associated parameterizations. Similarly, each RCP differs in its trajectory of radiative forcing due to greenhouse gas emissions and the final radiative forcing at the end of century. Therefore, each GCM–RCP combination reaches 1.5 °C, 2.0 °C and 3.0 °C increase in global mean temperature in different time periods. We identify 30-year periods for each GCM–RCP combination that result in different target warming levels [Supplementary Table 1]. Various GCM–RCP combinations reach the global mean temperature increase of 1.5 °C, 2.0 °C, and 3.0 °C between 2004 and 2047, 2016 and 2060, and 2035 and 2067, respectively. Note that for 10 out of 45 GCM–RCP combinations, we could not identify any 30-year period for selected warming levels. This was mainly observed with the RCP2.6 scenarios under the 3 °C warming level. Thus, only 35 climate scenarios across various GCM–RCP combinations are possible, which combined with 5 SSPs result in a 175 (instead of 225) total GCM–RCP–SSP combinations for estimating PCWA for each district. We estimate the changes in *P* and *PET* for each district across GCM–RCP combinations for each warming scenario [Fig. 2]. The median change across all GCM–RCP combinations is shown using color and the degree of agreement in the nature of change (increase or decrease) is indicated using transparency levels [Fig. 2a–c]. *P* is projected to increase under 1.5 °C warming for 95.8% of districts, but 90% of these increases are < 10% [Fig. 2a]. Only the northern Himalayan region is projected to witness a decrease in *P*, though these decreases are small, ranging

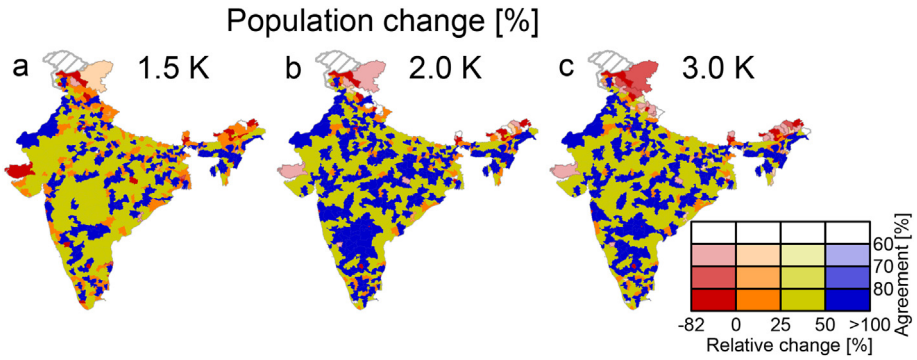

Fig. 3. Same as Fig. 2 but for projected changes in population as provided by 5 SSPs.

from 0.2% to 3.4%. Under 2.0 °C warming [Fig. 2b], the percentage of districts likely to undergo reductions in *P* increases to 69 (10.8%). The regions expecting reductions in *P* expand across the northern Himalayan regions including downstream plain regions, and few coastal districts on the western coast. The remaining parts of India are projected to witness a > 10% increase in precipitation for 2.0 °C warming levels.

Projections of *PET* have lesser spatial variations across all warming levels when compared with projections of *P* [Fig. 2d–f]. All GCM–RCP combinations project an increase in *PET*, in line with expected increases in temperature. Under 1.5 °C warming, median projected increases in *PET* stays below 10%. Under the 2.0 °C warming level, *PET* increases considerably for the northern and eastern parts of the Himalayas, and continues to increase under the 3.0 °C warming level.

Population projections suggest an overall increase from 1.5 °C to 2.0 °C warming levels, and stabilization between 2.0 °C and 3.0 °C warming levels [Fig. 3]. Across all districts and SSPs, the median of relative change in population from the year 2001 is 37.3%, 46.7%, and 45.5% for 1.5 °C, 2.0 °C, and 3.0 °C warming levels, respectively. As we transition from 2.0 °C to 3.0 °C warming, population decreases across 75.1% districts, though the magnitude of reduction is small (median: 1.8%, inter–quartile range: 1.5%). Thus, between 2.0 °C and 3.0 °C warming, population tends to stabilize but *P* becomes increasingly variable. Note that the uncertainty in population projections across SSPs are relatively small as compared to those for *P* projections. There is a high (> 80%) agreement between various SSPs regarding the nature of change in population for > 90% of the districts for each warming scenario.

3.2. Per capita water availability (PCWA) under 1.5 °C, 2.0 °C, and 3.0 °C

We employ the probabilistic Budyko model to estimate median values of PCWA across various climate and population change scenarios. PCWA is projected to decrease across all warming levels over majority of India [Fig. 4], when compared to the historical period. Under 1.5 °C warming, 92.3% of districts are projected to witness a reduction in PCWA. The projected decrease lies between 0–15%, 15–30%, and > 30% for 14.3%, 51.6%, and 26.4% of districts, respectively. The number of districts with large (> 30%) reductions in PCWA are higher (41.8%) under 2.0 °C warming. This indicates considerably greater water stress under 2.0 °C warming when compared to the 1.5 °C warming. A transition from 2.0 °C to 3.0 °C warming results in an increase in PCWA for 93.0% districts. However, considerable number of districts (43.3%) are projected to experience 15–30% reductions in PCWA even under 3.0 °C warming. There is a concurrent increase in the spatial variability of changes in PCWA from 2.0 °C to 3.0 °C warming.

The uncertainty in PCWA projections arising from various GCM–RCP–SSP combinations are similar under both 1.5 °C and 2.0 °C warming levels. However, 3.0 °C warming entails an increase in uncertainty, with 8.3% districts not agreeing on the direction of change in PCWA (compared to 2.3% under 1.5 °C and 2.0 °C warming). The regions where uncertainty increases under 3.0 °C warming are concentrated in inland parts of southern India, which is already water scarce. Overall, 61.2%, 62.9%, and 61.4% of districts have a strong (> 80%) agreement on the nature of change for 1.5 °C, 2.0 °C, and 3.0 °C warming levels, respectively.

Further discussion on how changes in *P*, *PET* and population are related to projected changes in PCWA is provided in Supplementary Text S1.

3.3. Sensitivity analysis

We find that for majority of districts, PCWA is most sensitive either to changes in population or *P* [Fig. 5]. Changes in *PET* generally have lowest sensitivity values among the three factors. Across all districts, the sensitivity index (median KS–Statistic) ranges from 0.23–0.82, 0.18–0.66, and 0.27–0.88 for *P*, *PET*, and population changes,

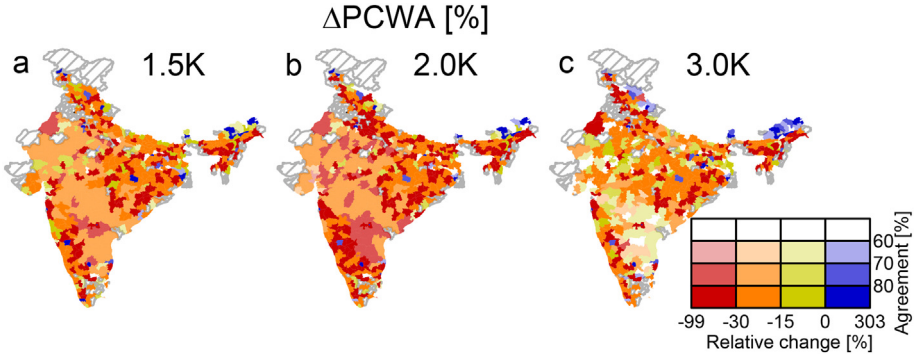

Fig. 4. Same as Fig. 2 but for projected changes in the median of PCWA as estimated by the probabilistic Budyko framework using climate and population projections for time periods with 1.5 °C, 2.0 °C, and 3.0 °C rise in global mean temperature. The baseline period for estimating relative change is 1971–2000.

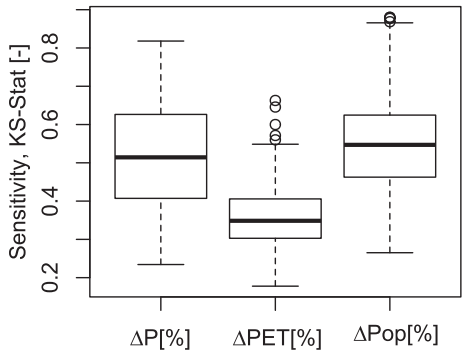

Fig. 5. Ranges of sensitivity index quantified via the median KS–Statistic (x-axis) for changes in long–term precipitation (*P*), potential evapotranspiration (*PET*) and population (Pop). The boxplot shows the median and the inter-quartile range of the sensitivity index across all districts with available data. Greater values indicate greater sensitivity of PCWA to a given factor.

respectively. Recall that higher values of the index indicate greater sensitivity. The median (inter-quartile range) of index is 0.51 (0.22), 0.35 (0.10), and 0.55 (0.16) for *P*, *PET*, and population changes, respectively.

We observe that when PCWA is most sensitive to *P* changes in a region, it is less sensitive to population changes. This is evident by a strong negative correlation between the sensitivity indices for *P* and population changes across districts (-0.64, p–value < 0.01). Additionally, there is a weak positive correlation between sensitivity indices for *P* and *PET* changes (0.33, p–value < 0.01) and a negative correlation between sensitivity indices for *PET* and population changes (-0.53, p–value < 0.01). Thus, when PCWA is more sensitive to *P* changes, it is also more sensitive to *PET* changes [Supplementary Fig. S3].

Interesting patterns are observed on visualizing the relative importance of factors spatially [Fig. 6]. For each district, the rank of each factor according to their sensitivity index is shown in Fig. 6. We find that changes in *P* have the highest sensitivity in western, midwestern, and southeastern regions. Northeastern regions, northern Himalayan regions, and southwestern coastal regions are most sensitive to increases in population. Overall, there are 249 (46.9%), 11 (2.1%), and 271 (51.0%) districts for which PCWA is most sensitive to changes in *P*, *PET*, and population, respectively.

Regions where population change is the most important factor have relatively low aridity indices and low population in the historical time period [Fig. 7]. These regions have a median aridity index of 1.2. Almost all districts with very low historical populations (< 0.5 million) show population change as the most dominant factor. Similarly, regions with historically lower *PET* tend to be most sensitive to population changes. Thus, the future sensitivity of PCWA for a region seems to depend on its historical climatic and demographic setting.

4. Discussion

We find that the categorization of a region's water stress based on absolute values of PCWA does not change much as we move across different warming scenarios [Fig. 8 and Supplementary Fig. S4]. Typically, values < 500 $m^3/year/capita$ are assumed to indicate high levels of water scarcity, while values > 1700 $m^3/year/capita$ indicate water sufficiency. Intermediary values indicate varying levels of water stress often distinguished by the 1000 $m^3/year/capita$ threshold. Overall, 354, 421, and 380 million people are likely to face severe water stress (PCWA < 500 $m^3/year/capita$) under 1.5 °C, 2.0 °C, and 3.0 °C warming levels, respectively. Also, 261, 256, and 270 million people are likely to remain water sufficient ($> 1700 m^3/year/capita$) under 1.5 °C, 2.0 °C, and 3.0 °C warming levels, respectively. The number of people under water stress are greater than those under water sufficient conditions at all warming levels.

The approach employed for assessing future water availability depends mainly on the availability of ground-based streamflow data and the temporal scale of the hydrologic indicator that needs to be predicted. In our analysis, we aimed to predict long–term water availability, which can be predicted with reasonable accuracy using the parsimonious Budyko model. Our method provides a long–term hydrologic budget at relatively fine spatial resolution of decision-relevant unit (a political unit) in absence of naturalized streamflow [Singh and Kumar, 2015]. On comparing our results with studies that utilize complex hydrologic models, we find a reasonable agreement among projected changes in renewable freshwater [Schewe et al., 2014; Gosling et al., 2017].

Under 3.0 °C warming, our analysis as well as Schewe et al. (2014) project strong and certain increases in renewable freshwater for southern India and a reduction northern Himalayan region [Supplementary Fig. S5]. In fact, the magnitude of change is also similar for both regions. The only region for which our analysis projects a different outcomes from Schewe et al. (2014) is the western desert region. Using several hydrologic models, Schewe et al. (2014) project large uncertainties for this region but the Budyko model projects a certain increase in freshwater availability. A likely cause of this difference is that hydrological models, from low to moderate complexity, are unable to capture the hydrological processes adequately in very arid environments. Similarly, Gosling et al. (2017) report an expected increase of $> 20\%$ in mean annual runoff for the Ganges basin under 3.0 °C warming. The Budyko framework shows a projected increase between 10 and 30% for most of the Ganges basin.

Another approach to estimate changes in freshwater availability in a region is to directly use raw GCM outputs of $P - AET$ [Xu et al., 2005]. This approach was recently appraised by Padrón et al. (2018) at a global scale, who showed that raw GCM outputs generally project more extreme changes when compared to observationally constrained GCM outputs. We find similar results using our GCM based $P - AET$ datasets. The 30–year mean annual $P - AET$ estimated from the Budyko model forced with downscaled and bias-corrected GCM climate data projects less extreme changes when compared to raw GCM projected $P - AET$ [Supplementary Fig. S6-S7]. Additionally, the historical estimates of

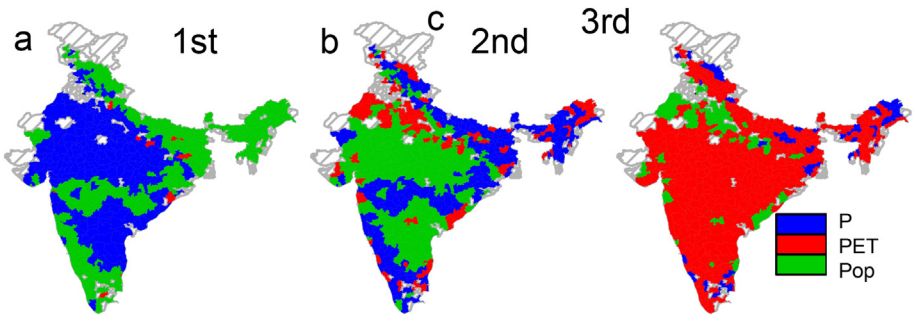

Fig. 6. Relative importance of changes in long–term precipitation (*P*, blue), long–term potential evapotranspiration (*PET*, red), and population (POP, green) across all districts in India where data was available. The spatial distribution of factors with a) first, b) second, and c) third highest sensitivity index is shown. (For interpretation of the references to color in this figure legend, the reader is referred to the web version of this article.)

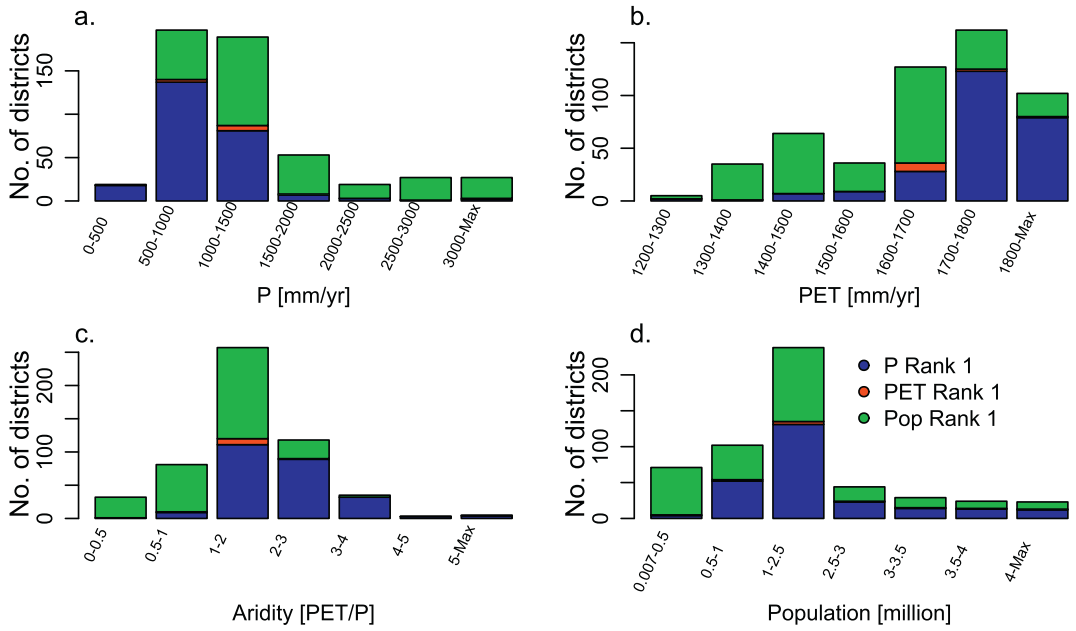

Fig. 7. The relative importance of *P*, *PET*, and population in controlling PCWA. Each panel shows the importance of a factor across the range of historical values of a) *P*, b) *PET*, c) aridity index (*PET*/*P*), and d) population. In each panel, the length of a colored vertical bar (y-axis) denotes the number of districts for which the particular factor ranked first: blue for *P*, red for *PET*, and green for population. (For interpretation of the references to color in this figure legend, the reader is referred to the web version of this article.)

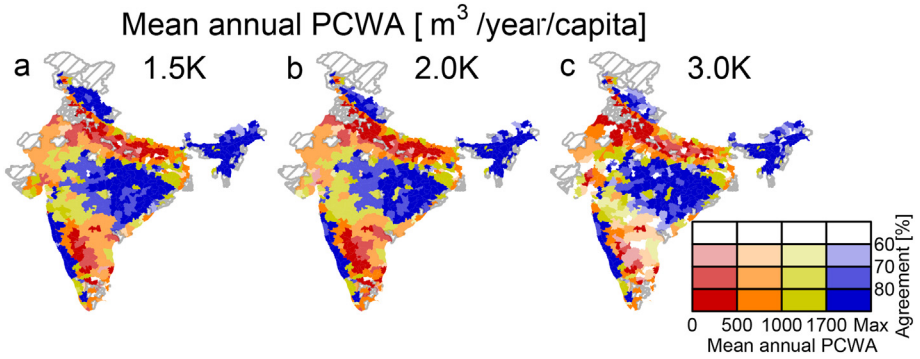

Fig. 8. Same as Fig. 2 but for projected estimates of PCWA.

P − *AET* obtained from the Budyko model forced with downscaled and bias-corrected GCM climate data is in closer agreement with those obtained from observationally forced Budyko model, when compared to raw GCM projected *P* − *AET* [Supplementary Fig. S8].

Several sources of uncertainty affect future estimates of renewable freshwater resources in a region such as those from choice of GCM, RCP, hydrologic model and its parameterization [Schewe et al., 2014]. GCMs are a significant source of uncertainty in estimating future water availability, particularly for monsoon dominated regions such as India [Ashfaq et al., 2017; Chen and Zhou, 2015; Saha et al., 2014]. In our analysis, we found that the uncertainty from GCM structure varies based on the warming level and RCP scenario [Supplementary Figs. S9-S10]. As compared to uncertainty in *P*, uncertainty in projections of *PET* are quite small. Furthermore, uncertainty across RCPs for different GCMs is much smaller as compared to uncertainty across GCMs for each RCP. Finally, additional uncertainty stems from the presence of decadal oscillations in Indian monsoonal rainfall, which may affect estimates of long–term changes in *P* and *PET* [Zhang et al., 2018]. Though using a 30-year window to identify a given warming level likely reduces the impact of decadal oscillations, as compared to those that consider a 9-year window as in Zhang et al. (2018), this effect should be explored studies.

We have already established that for estimating long–term water availability, the Budyko model is a suitable candidate. Historical uncertainty in parameterization of the Budyko curve is considered in the probabilistic version of the model, but it is not further considered for the sensitivity analysis. ω varies from 1.1–5.6 across all districts units with a median (inter–quartile range) of 1.5 (0.4). The median (inter-quartile range) of regionally grouped ω values are 1.7 (0.3), 1.4 (0.2), 1.4 (0.1), and 1.9 (0.6) for northern, eastern, western, and southern regional divisions, respectively [see Supplementary Text S2 for further details]. Uncertainty also stems from variation of ω with time, which is not considered here for two reasons. First, a number of studies have already proposed analytical or numerical approaches to quantify the sensitivity of Budyko projected water availability to changes in ω and *PET*/*P* (see Gudmundsson et al. (2016) and references therein). Second, our sensitivity analysis method relies on identifying possible future changes in independent variables. Thus, to understand the sensitivity of water availability to changes in ω, we need a method that can predict how ω may change in the future for each district. Kumar et al. (2016) provide a global scale GCM based analysis of possible changes in ω in the future. However, their analysis was carried out with coarse resolution GCM data. Given the issues with raw GCM data to adequately reproduce the historical estimates of water availability as discussed

earlier, we have opted here to not to explore possible effects of changes in ω in the future. Thus, characterizing future uncertainty in ω is an important area to be explored in future work.

Our estimates of freshwater availability are conditioned on a hydro-climatic database and as such they do not consider the role of technology in enabling access to water, water quality issues, and temporal variability of water supply. Global scale analyses have shown that these additional factors further constrain water availability [van Vliet et al., 2017]. Uncertainties are also introduced due to the choice of method used for estimating *PET* from temperature data [Milly and Dunne, 2016]. More physically based estimation methods may provide accurate estimates but require greater data support. We also ignore the role of deeply mined groundwater in alleviating water stress, by focusing only on renewable shallow groundwater. This assumption does not take away from the utility of this analysis as many parts of India are already at their limits of groundwater abstraction and perhaps it is prudent to estimate and plan for renewable water resources [Wada et al., 2012; Anantha, 2013; Lapworth et al., 2014].

5. Conclusions

Preventing a transition from 1.5 °C to 2.0 °C global warming levels is likely advantageous due to the certainty of reduction in per capita water availability under 2.0 °C warming. We find that the number of people likely to face severe water scarcity (PCWA < 500 $m^3/year/capita$) increase from 354 million to 421 million as we transition from 1.5 °C to 2.0 °C warming levels. We also conclude that it is not just climatic changes that will govern the future of water availability in India but also population changes. Using SSPs that depict likely changes in population, we show that despite certainty of precipitation increase under 3.0 °C warming, water availability remains uncertain or decreases as compared to the historical baseline due to compensatory role of population increase.

The sensitivity analysis revealed interesting spatial patterns of relative importance of climate and population in controlling PCWA. Changes in PCWA are driven by both population increases and mean annual precipitation changes, while changes in mean annual potential evapotranspiration plays a secondary role. Thus, it revealed that temperature change itself is not a major driver of water stress, precipitation change is. Also, we show that population change plays a major role in controlling water stress in many regions, an observation confirmed by previous studies. Our main contribution is to show that the factor that dominates most in a region depends upon the regions historical climatic and population settings, an observation previously unexplored. Areas with relatively lower populations and greater historical PCWA tend to be more sensitive to population changes, while others are more sensitive to precipitation changes. This indicates that policies need to account for the possibility that each region is unique and will respond to initiatives depending upon its own climatic and socio-economic history. Thus, socio-economic policies will have an important role to play alongside policies related to climate change abatement in determining the future of water security in India.

Our analysis highlights the complex interactions of population growth, rising temperatures and changing precipitation that influence future water availability. In most cases, projected increases in precipitation do not translate directly to increasing per capita water availability, as they are offset by increasing temperature and population. Despite considerable spatial variability in the projected changes, there is a strong agreement among GCM–RCP–SSP combinations that over majority of India PCWA will decrease in the future. Our analyses only considered freshwater available in rivers and shallow groundwater, generally termed as blue water. Further analyses need to consider the role of green water (water transpired by plants) and virtual water trade (water embedded in products) in affecting water availability.

Appendix A. Supplementary data

Supplementary data to this article can be found online at https://doi.org/10.1016/j.gloplacha.2019.03.006.

References

Anantha, K., 2013. Economic implications of groundwater exploitation in hard rock areas of southern peninsular India. Environ. Dev. Sustain. 15 (3), 587–606.

Arnell, N.W., 2004. Climate change and global water resources: SRES emissions and socio-economic scenarios. Glob. Environ. Chang. 14 (1), 31–52.

Arnell, N.W., Lloyd-Hughes, B., 2014. The global-scale impacts of climate change on water resources and flooding under new climate and socio-economic scenarios. Clim. Chang. 122 (1–2), 127–140.

Ashfaq, M., Rastogi, D., Mei, R., Touma, D., Leung, L.R., 2017. Sources of errors in the simulation of south asian summer monsoon in the CMIP5 GCMs. Clim. Dyn. 49 (1–2), 193–223.

Budyko, M., 1958. The Heat Balance of the Earth's Surface. National Weather Service, U.S Department of Commerce, Washington D.C.

Chen, X., Zhou, T., 2015. Distinct effects of global mean warming and regional sea surface warming pattern on projected uncertainty in the south asian summer monsoon. Geophys. Res. Lett. 42 (21), 9433–9439.

Döll, P., Schmied, H.M., 2012. How is the impact of climate change on river flow regimes related to the impact on mean annual runoff? A global-scale analysis. Environ. Res. Lett. 7 (1), 014037.

Donnelly, C., Greuell, W., Andersson, J., Gerten, D., Pisacane, G., Roudier, P., Ludwig, F., 2017. Impacts of climate change on European hydrology at 1.5, 2 and 3 degrees mean global warming above preindustrial level. Clim. Chang. 143 (1–2), 13–26.

Fu, B., 1981. On the calculation of the evaporation from land surface (in chinese). Sci. Atmos. Sin. 5, 23–31.

Gerten, D., Heinke, J., Hoff, H., Biemans, H., Fader, M., Waha, K., 2011. Global water availability and requirements for future food production. J. Hydrometeorol. 12 (5), 885–899.

Gosling, S.N., Arnell, N.W., 2016. A global assessment of the impact of climate change on water scarcity. Clim. Chang. 134 (3), 371–385.

Gosling, S.N., Zaherpour, J., Mount, N.J., Hattermann, F.F., Dankers, R., Arheimer, B., Breuer, L., Ding, J., Haddeland, I., Kumar, R., et al., 2017. A comparison of changes in river runoff from multiple global and catchment-scale hydrological models under global warming scenarios of 1°C, 2°C and 3°C. Clim. Chang. 141 (3), 577–595.

Greve, P., Gudmundsson, L., Orlowsky, B., Seneviratne, S.I., 2015. Introducing a probabilistic Budyko framework. Geophys. Res. Lett. 42 (7), 2261–2269. https://doi.org/10.1002/2015GL063449.

Gudmundsson, L., Greve, P., Seneviratne, S.I., 2016. The sensitivity of water availability to changes in the aridity index and other factors-a probabilistic analysis in the Budyko space. Geophys. Res. Lett. 43 (13), 6985–6994.

Haddeland, I., Heinke, J., Biemans, H., Eisner, S., Flörke, M., Hanasaki, N., Konzmann, M., Ludwig, F., Masaki, Y., Schewe, J., et al., 2014. Global water resources affected by human interventions and climate change. Proc. Natl. Acad. Sci. 111 (9), 3251–3256.

Hargreaves, G., Samani, Z., 1985. Reference crop evapotranspiration from temperature. Trans. ASAE 1, 96–99.

Hempel, S., Frieler, K., Warszawski, L., Schewe, J., Piontek, F., 2013. A trend-preserving bias correction - the ISI–MIP approach. Earth Syst. Dyn. 4 (2), 219–236. http://www.earth-syst-dynam.net/4/219/2013/.

Jacob, D., Kotova, L., Teichmann, C., Sobolowski, S.P., Vautard, R., Donnelly, C., Koutroulis, A.G., Grillakis, M.G., Tsanis, I.K., Damm, A., et al., 2018. Climate impacts in Europe under +1.5°C global warming. Earth's Future 6 (2), 264–285.

Jones, B., O'Neill, B., 2016. Spatially explicit global population scenarios consistent with the shared socioeconomic pathways. Environ. Res. Lett. 11 (8), 084003.

Jones, B., O'Neill, B., 2017. Global Population Projection Grids Based on Shared Socioeconomic Pathways (ssps), 2010–2100. NASA Socioeconomic Data and Applications Center (SEDAC), Palisades, NY. https://doi.org/10.7927/H4RF5S0P. Accessed 04/07/2018.

Krysanova, V., Hattermann, F.F., 2017. Intercomparison of climate change impacts in 12 large river basins: overview of methods and summary of results. Clim. Chang. 141 (3), 363–379.

Kumar, S., Zwiers, F., Dirmeyer, P.A., Lawrence, D.M., Shrestha, R., Werner, A.T., 2016. Terrestrial contribution to the heterogeneity in hydrological changes under global warming. Water Resour. Res. 52 (4), 3127–3142.

Kummu, M., Guillaume, J., de Moel, H., Eisner, S., Flörke, M., Porkka, M., Siebert, S., Veldkamp, T., Ward, P., 2016. The world's road to water scarcity: shortage and stress in the 20th century and pathways towards sustainability. Sci. Rep. 6.

Lapworth, D., Gopal, K., Rao, M., MacDonald, A., 2014. Intensive Groundwater Exploitation in the Punjab: An Evaluation of Resource and Quality Trends.

Marx, A., Kumar, R., Thober, S., Rakovec, O., Wanders, N., Zink, M., Wood, E.F., Pan, M., Sheffield, J., Samaniego, L., 2018. Climate change alters low flows in Europe under global warming of 1.5, 2, and 3°C. Hydrol. Earth Syst. Sci. 22 (2), 1017–1032.

McSweeney, C.F., Jones, R.G., 2016. How representative is the spread of climate projections from the 5 CMIP5 GCMs used in ISI-MIP? Clim. Serv. 1, 24–29.

Mekonnen, M.M., Hoekstra, A.Y., 2016. Four billion people facing severe water scarcity. Sci. Adv. 2 (2), e1500323.

Milly, P.C., Dunne, K.A., 2016. Potential evapotranspiration and continental drying. Nat. Clim. Chang. 6 (10), 946.

Milly, P.C., Dunne, K.A., Vecchia, A.V., 2005. Global pattern of trends in streamflow and water availability in a changing climate. Nature 438 (7066), 347.

Mishra, V., Kumar, R., Shah, H.L., Samaniego, L., Eisner, S., Yang, T., 2017. Multimodel assessment of sensitivity and uncertainty of evapotranspiration and a proxy for available water resources under climate change. Clim. Chang. 141 (3), 451–465.
Padrón, R.S., Gudmundsson, L., Seneviratne, S.I., 2018. Observational constraints reduce likelihood of extreme changes in multi-decadal land water availability. Geophys. Res. Lett. 46 (2), 736–744.
Pianosi, F., Wagener, T., 2015. A simple and efficient method for global sensitivity analysis based on cumulative distribution functions. Environ. Model. Softw. 67, 1–11.
Pike, J., 1964. The estimation of annual runoff from meteorological data in a tropical climate. J. Hydrol. 2, 116–123.
Rockström, J., Steffen, W.L., Noone, K., Persson, Å., Chapin III, F.S., Lambin, E., Lenton, T.M., Scheffer, M., Folke, C., Schellnhuber, H.J., et al., 2009. Planetary Boundaries: Exploring the Safe Operating Space for Humanity.
Rodell, M., Famiglietti, J., Wiese, D., Reager, J., Beaudoing, H., Landerer, F., Lo, M.-H., 2018. Emerging trends in global freshwater availability. Nature 1.
Saha, A., Ghosh, S., Sahana, A., Rao, E., 2014. Failure of CMIP5 climate models in simulating post-1950 decreasing trend of Indian monsoon. Geophys. Res. Lett. 41 (20), 7323–7330.
Samaniego, L., Thober, S., Kumar, R., Wanders, N., Rakovec, O., Pan, M., Zink, M., Sheffield, J., Wood, E., Marx, A., 2018. Anthropogenic warming exacerbates European soil moisture droughts. Nat. Clim. Chang. 8 (5), 421.
Schewe, J., Heinke, J., Gerten, D., Haddeland, I., Arnell, N.W., Clark, D.B., Dankers, R., Eisner, S., Fekete, B.M., Colón-González, F.J., et al., 2014. Multimodel assessment of water scarcity under climate change. Proc. Natl. Acad. Sci. 111 (9), 3245–3250.
Schleussner, C.-F., Rogelj, J., Schaeffer, M., Lissner, T., Licker, R., Fischer, E.M., Knutti, R., Levermann, A., Frieler, K., Hare, W., 2016. Science and policy characteristics of the Paris Agreement temperature goal. Nat. Clim. Chang. 6 (9), 827.
Singh, R., Kumar, R., 2015. Vulnerability of water availability in India due to climate change: a bottom-up probabilistic Budyko analysis. Geophys. Res. Lett. 42 (22), 9799–9807.
Thober, S., Kumar, R., Wanders, N., Marx, A., Pan, M., Rakovec, O., Samaniego, L., Sheffield, J., Wood, E.F., Zink, M., 2018. Multi-model ensemble projections of European river floods and high flows at 1.5, 2, and 3 degrees global warming. Environ. Res. Lett. 13 (1), 014003.
van Vliet, M.T., Flörke, M., Wada, Y., 2017. Quality matters for water scarcity. Nat. Geosci. 10 (11), 800.
Vautard, R., Gobiet, A., Sobolowski, S., Kjellström, E., Stegehuis, A., Watkiss, P., Mendlik, T., Landgren, O., Nikulin, G., Teichmann, C., et al., 2014. The European climate under a 2°C global warming. Environ. Res. Lett. 9 (3), 034006.
Vörösmarty, C.J., Green, P., Salisbury, J., Lammers, R.B., 2000. Global water resources: vulnerability from climate change and population growth. science 289 (5477), 284–288.
Vörösmarty, C.J., McIntyre, P.B., Gessner, M.O., Dudgeon, D., Prusevich, A., Green, P., Glidden, S., Bunn, S.E., Sullivan, C.A., Liermann, C.R., et al., 2010. Global threats to human water security and river biodiversity. Nature 467 (7315), 555.
Wada, Y., Beek, L., Bierkens, M.F., 2012. Nonsustainable groundwater sustaining irrigation: a global assessment. Water Resour. Res. 48 (6).
Warszawski, L., Frieler, K., Huber, V., Piontek, F., Serdeczny, O., Schewe, J., 2014. The Inter-Sectoral Impact Model Intercomparison Project (ISI–MIP): Project framework. Proc. Natl. Acad. Sci. 111 (9), 3228–3232.
Water, U.N., 2007. Coping with Water Scarcity: Challenge of the Twenty-First Century. Prepared for World Water Day.
Wiltshire, A., Gornall, J., Booth, B., Dennis, E., Falloon, P., Kay, G., McNeall, D., McSweeney, C., Betts, R., 2013. The importance of population, climate change and co 2 plant physiological forcing in determining future global water stress. Glob. Environ. Chang. 23 (5), 1083–1097.
Xu, H., Wu, M.M., 2017. Water availability indices–a literature review. Tech. rep. https://doi.org/10.2172/1348938. https://www.osti.gov/biblio/1348938 Argonne National Lab.(ANL), Argonne, IL (United States), ANL/ESD-17/5.
Xu, C.-y., Widén, E., Halldin, S., 2005. Modelling hydrological consequences of climate change-progress and challenges. Adv. Atmos. Sci. 22 (6), 789–797.
Zhai, R., Tao, F., Xu, Z., 2018. Spatial–temporal changes in runoff and terrestrial ecosystem water retention under 1.5 and 2°c warming scenarios across China. Earth Syst. Dyn. 9 (2), 717.
Zhang, L., Hickel, K., Dawes, W.R., Chiew, F.H.S., Western, A.W., Briggs, P.R., 2004. A rational function approach for estimating mean annual evapotranspiration. Water Resour. Res. 40 (2), W02502 URL. https://doi.org/10.1029/2003WR002710.
Zhang, K., Kimball, J.S., Mu, Q., Jones, L.A., Goetz, S.J., Running, S.W., 2009. Satellite based analysis of northern {ET} trends and associated changes in the regional water balance from 1983 to 2005. J. Hydrol. 379 (1–2), 92–110. http://www.sciencedirect.com/science/article/pii/S0022169409006210.
Zhang, W., Zhou, T., Zou, L., Zhang, L., Chen, X., 2018. Reduced exposure to extreme precipitation from 0.5°c less warming in global land monsoon regions. Nat. Commun. 9 (1), 3153.